Desalination and Water Treatment
www.deswater.com
doi: 10.1080/19443994.2014.937752

55 (2015) 2155–2164
August

Taylor & Francis
Taylor & Francis Group

Degradation of acephate by colloidal manganese dioxide in the absence and presence of surfactants

Qamruzzaman, Abu Nasar*

Faculty of Engineering and Technology, Department of Applied Chemistry, Aligarh Muslim University, 202 002 Aligarh, India, Tel. +91 9369989605; Fax: +91 0571 2700528; email: qamar.phy@gmail.com (Qamruzzaman), Tel. +91 05712700920; email: abunasaramu@gmail.com (A. Nasar)

Received 24 September 2013; Accepted 31 May 2014

ABSTRACT

The kinetics of the degradation of acephate by water-soluble colloidal MnO_2 in acidic medium ($HClO_4$) has been studied spectrophotometrically in the absence and presence of surfactants. The experiments have been performed under the pseudo-first-order reaction conditions with respect to MnO_2. The degradation has been observed to be fractional order with respect to acephate and $HClO_4$ while first order with respect to MnO_2 in the absence and presence of surfactants. It has been observed that cationic surfactant, cetyl trimethyl ammonium bromide, causes flocculation with oppositely charged colloidal MnO_2 whereas anionic surfactant, sodium dodecyl sulfate, has no considerable effect on the reaction kinetics. However, non-ionic surfactant, Triton X-100 (TX-100) accelerates the reaction rate. The catalytic effect of TX-100 has been discussed in the light of the available mathematical model. The kinetic data have been used to calculate the different activation parameters for the oxidative degradation of acephate by colloidal MnO_2.

Keywords: Degradation; Acephate; Manganese dioxide; Pseudo-first-order; Surfactants; TX-100

1. Introduction

Acephate (O,S-dimethyl acetylphosphoramidothioate) is one of the most important organophosphorus pesticides commonly used for the insecticidal activity. It is highly effective against a number of insect pests, such as aphids, thrips, leaf miners, sawflies, and lepidopterous larvae etc. [1]. It acts by inhibiting acetylcholinesterase activity in insects and widely used to protect a variety of agricultural and ornamental arenas. However, acephate and its first metabolite, methamidophos (O,S-dimethyl phosphoramidothioate) have been observed to be toxic to various species [2–8]. Furthermore, organophosphorus pesticides have been considered as common organic pollutants because they have potential to contaminate the ground water and have adverse effects on environmental safety [9–14]. Accordingly, increasing use of these insecticides in the agricultural field is associated with the significant risk to water resources and aquatic systems. Thus, degradation of such compounds in soil, after fulfillment of their insecticidal role, is essential to eliminate or minimize the contamination of water resources. Therefore, there is an urgent need to develop an efficient and economical method for the degradation of acephate which would be helpful in

*Corresponding author.

the treatment of wastewater contaminated by it. In fact, the fate of an insecticide in soil is governed by the transformation process based on the splitting of molecules which includes photochemical, biological, and chemical degradations. During recent years, heterogeneous photocatalytic degradation of acephate in aqueous TiO_2 suspensions has been extensively investigated [15–19]. Biodegradation investigations of acephate [20] and its first metabolic product i.e. methamidophos [21] have also been reported. Chai et al. [22] have studied the effect of soil moisture, temperature, microbial activity, and application rate on acephate degradation in soils and also examined and identified the critical variables determining its degradation kinetics.

Furthermore, it is well known that many pesticides and other organic substances undergo chemical decomposition in the presence of manganese compounds and especially its dioxide (MnO_2). In fact, manganese is 12th most abundant element in earth's crust and available in variable amounts depending upon region and location. The MnO_2 particles present in earth's crust and natural water have potential for oxidative degradation of humic and organic substances, including pesticides. However, oxidizing power of MnO_2 is limited due to its insolubility under ordinary conditions. Fortunately, in recent years perfectly transparent colloidal solution of MnO_2 has been prepared by reducing potassium permanganate solution by sodium thiosulfate. The water soluble form of colloidal MnO_2 is advantageous over its insoluble form due to higher oxidizing power and feasibility of monitoring the reaction by conventional UV–visible spectrophotometry. The water-soluble colloidal MnO_2 has successfully been used for the oxidation studies of a number of pesticides and other organic compounds such as formic acid [23,24], D-fructose [25], D-glucose [26], glycyl–glycine [27], glycolic acid [28], DL-malic acid [29], mandelic acid [30], metribuzin [31], L-methionine [32], oxalic acid [33,34], thiourea [35], tricyclazole [36], etc. by employing UV–visible spectrophotometric technique. As, so far, the degradation of acephate by colloidal MnO_2 has not been studied, it has been considered worth to conduct measurements in this direction. In the present study, the degradation kinetics of acephate by water-soluble synthetic colloidal MnO_2 in acidic medium ($HClO_4$) has been performed. Since surfactants are commonly used in pesticide formulation to increase the solubility of pesticides and also to enhance their effectiveness by fine spray, it was also considered worth to extend the study in presence of common surfactants such as cetyl trimethyl ammonium bromide (CTAB), sodium dodecyl sulfate (SDS), and Triton X-100 (TX-100). Selection of these surface active agents is based on the criteria of picking one member from each category of cationic, anionic, and non-ionic compounds as chosen in the respective order. The kinetic data have been analyzed in the light of Arrhenius and Eyring theories and different activation parameters have also been determined.

2. Experimental

2.1. Materials

Commercial grade acephate (>97%) obtained from Excel Crop Care, India available under the trade name of ACEfEX was used as received for the preparation of solution. Scintillation grade TX-100 (CDH, India) and analytical reagent grade for each perchloric acid (Merck, Germany), CTAB (CDH, India), SDS (SRL, India) potassium permanganate, and sodium thiosulfate (Qualigens, India) were used in the present investigation. Following analytical reagent grade electrolytic salts: LiCl, NaCl, KCl, NH_4Cl, $MgCl_2$, $CaCl_2$, and $BaCl_2$ (each obtained from SRL, India) and $SrCl_2$ (CDH, India) were used for the characterization of colloidal MnO_2 solution. Doubly distilled deionized water was used throughout the experimental studies.

2.2. Preparation and characterization of colloidal MnO_2

The water-soluble colloidal MnO_2 solution was prepared by the method described by Perez-Benito and co-workers [23,34,37]. The preparation involves the reduction of potassium permanganate by sodium thiosulfate in aqueous medium according to the following stoichiometry, details of which have been described elsewhere [31,36]:

$$8MnO_4^- + 3S_2O_3^{2-} + 2H^+ \rightarrow 8MnO_2 + 6SO_4^{2-} + H_2O \quad (1)$$

The resulting solution was perfectly transparent dark brown and showed one broad band covering the wide region of UV–visible spectra (250–650 nm) with the $\lambda_{max} = 360$ nm. The fulfillment of Beer's law was checked at this wavelength and was found to be valid throughout the entire concentration range of MnO_2 (0.6×10^{-4}–1.6×10^{-4} mol dm^{-3}).

The formation of water-soluble colloidal particles of MnO_2 was checked by adding a minimum amount of different electrolytes, necessary for their precipitation [37]. For this purpose, appropriate amount of different types of electrolytes containing monovalent and

divalent cations, viz. LiCl, NaCl, KCl, NH_4Cl, $MgCl_2$, $CaCl_2$, $BaCl_2$, and $SrCl_2$ were mixed to the solution with stirring. With each electrolyte, appearance of precipitate in the reaction mixture was observed which indicated the presence of water-soluble form of colloidal particles of MnO_2. According to Perez-Benito et al. [37] the precipitation of MnO_2 is due to the adsorption of electrolytic cations on its negatively charged colloidal particles.

An alternative method based on the Rayleigh's scattering law was also used to further confirm the formation of colloidal particles. According to this law, the absorbance (A) due to scattering of light by a solution of colloidal particles is inversely proportional to the fourth power of the wavelength (λ) [38]. The plots between log A and log λ in the region ranges from 360 nm (λ_{max} for MnO_2) to 530 nm (λ_{max} for $KMnO_4$) were linear with slopes (between 4.19 and 4.26 depending upon the concentration of MnO_2), which were slightly greater than the theoretical value of 4.0. Thus, on the basis of above observations one can safely conclude that the water-soluble MnO_2 as prepared from $KMnO_4$ is in the form of colloidal particles.

2.3. Kinetic measurements

Kinetic experiments were performed by taking requisite quantity of aqueous solution of acephate in a reaction vessel kept in a thermostatized water bath. The reaction vessel was allowed to remain in the water bath for sufficient time to attain the desired temperature with an accuracy of ±0.5 °C. The kinetic studies were carried out by adding the calculated amount of colloidal solution of MnO_2, $HClO_4$, and surfactants, whenever required. The progress of the reaction was monitored spectrophotometrically. The absorbance of unreacted MnO_2 in the reaction mixture was taken by UV–visible spectrophotometer (Perkin Elmer, USA; Model—lambda 25) at an optimized wavelength of 360 nm (i.e. $\lambda_{max} = 360$ nm). The fulfillment of Beer's law was checked and found to be validated in experimental concentration range of MnO_2. The measurements were taken under the varying conditions of different concentrations of acephate (1.0×10^{-3}–1.0×10^{-2} mol dm^{-3}), MnO_2 (0.6×10^{-4}–1.6×10^{-4} mol dm^{-3}), $HClO_4$ (1.0×10^{-4}–1.2×10^{-3} mol dm^{-3}) surfactants (1.0×10^{-4}–5.0×10^{-3} mol dm^{-3}), and temperature (20–45 °C). The concentration range of acephate is selected in such a way that the pseudo-first-order reaction condition with respect to MnO_2 be maintained throughout the experiments.

3. Results and discussion

3.1. General consideration

All the measurements were formulated under the pseudo-first-order reaction conditions in which concentrations of acephate and $HClO_4$ were taken in large excess over MnO_2. The pseudo-first-order rate constants were calculated from the slope of log (absorbance) vs. time plot. The plot of log (absorbance) vs. time at typical fixed concentrations of acephate (5.0×10^{-3} mol dm^{-3}), MnO_2 (8.0×10^{-5} mol dm^{-3}), and $HClO_4$ (6.0×10^{-4} mol dm^{-3}) at 30 °C shown in Fig. 1 is represented by straight line with $r^2 = 0.989$. Thus, the reaction is first order with respect to MnO_2 under the adopted reaction conditions.

3.2. Effect of concentrations of acephate, MnO_2, and $HClO_4$ on the reaction rate

The dependence of the rate of reaction on the concentration of acephate has been studied by conducting the kinetic measurements at the varying concentration of acephate (1.0×10^{-3}–1.0×10^{-2} mol dm^{-3}) keeping the concentrations of MnO_2 (8.0×10^{-5} mol dm^{-3}) and $HClO_4$ (6.0×10^{-4} mol dm^{-3}) constant at a fixed temperature of 30 °C. Under the above-mentioned conditions, the values of observed rate constant (k_{obs}), so obtained, are plotted against the concentration of acephate in Fig. 2. This figure clearly indicates that the variation is non-linear and the rate constant increases with increasing concentration of acephate throughout the entire range of concentration. The plot between

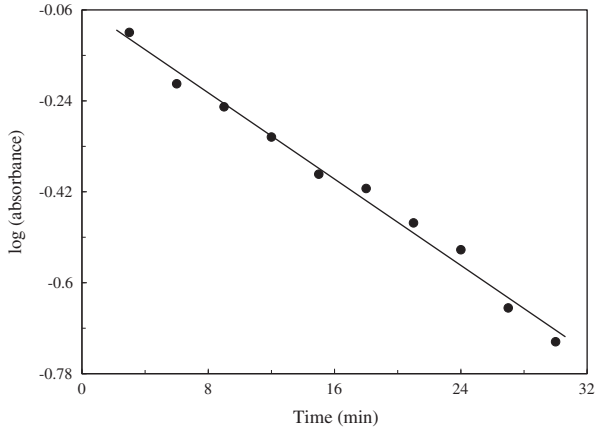

Fig. 1. Plot of log (absorbance) vs. time for the degradation of acephate by colloidal MnO_2 (Reaction conditions: [acephate] = 5.0×10^{-3} mol dm^{-3}, [MnO_2] = 8.0×10^{-5} mol dm^{-3}, [$HClO_4$] = 6.0×10^{-4} mol dm^{-3}, temperature = 30 °C).

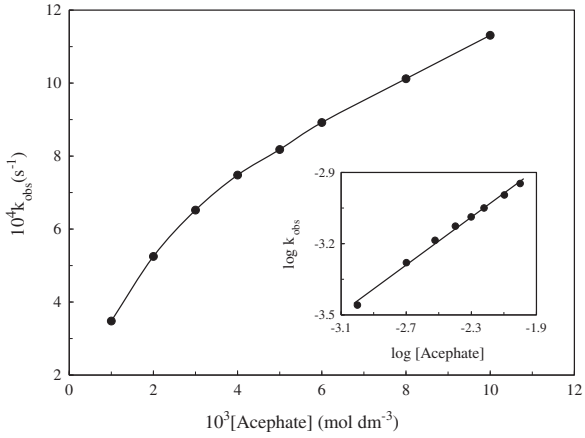

Fig. 2. Effect of [acephate] on k_{obs} (inset—log [acephate] on log k_{obs}) for the degradation of acephate by colloidal MnO_2 (Reaction conditions: $[MnO_2] = 8.0 \times 10^{-5}$ mol dm^{-3}, $[HClO_4] = 6.0 \times 10^{-4}$ mol dm^{-3}, temperature = 30 °C).

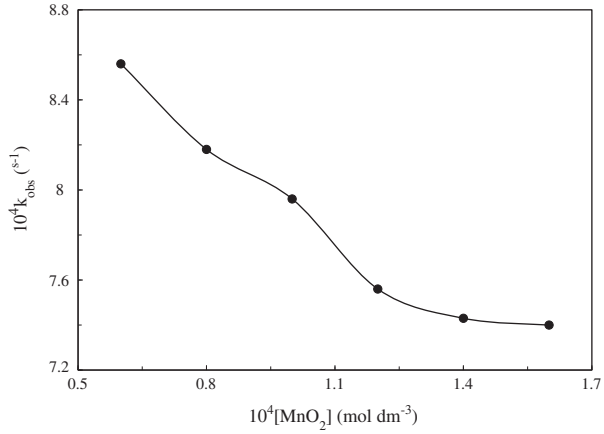

Fig. 3. Effect of $[MnO_2]$ on k_{obs} for the degradation of acephate by colloidal MnO_2 (Reaction conditions: [acephate] = 5.0×10^{-3} mol dm^{-3}, $[HClO_4] = 6.0 \times 10^{-4}$ mol dm^{-3}, temperature = 30 °C).

log k_{obs} and log [acephate] is linear (Fig. 2—inset) with a slope of 0.503 ($r^2 = 0.995$), indicating the fractional order with respect to acephate. In this context, it is worth relevant to notice that the oxidative degradation of similar pesticides, namely, metribuzin [31] and tricyclazole [36] by colloidal MnO_2 in acidic medium, has also been observed to obey fractional-order reaction kinetics. These findings are also in conformity with the observation of fractional order for the oxidative degradation of a number of other organic compounds, such as D-fructose [25], glycyl–glycine [27], glycolic acid [28], thiourea [35], etc. under similar conditions.

In order to understand the nature of reaction with respect to variation in concentration of MnO_2, the rate constants have been determined at different initial concentrations of MnO_2 ranging from 6.0×10^{-5} to 1.6×10^{-4} mol dm^{-3}. The concentrations of acephate (5.0×10^{-3} mol dm^{-3}) and $HClO_4$ (6.0×10^{-4} mol dm^{-3}) and temperature (30 °C) have been kept constants. The pseudo-first-order rate constant obtained at different concentrations of MnO_2 is plotted in Fig. 3. This figure clearly shows that there is continuous decrease in rate constant with the increasing concentration of MnO_2. However, the change is more pronounced in lower concentrations of MnO_2 (i.e. up to 1.2×10^{-4} mol dm^{-3}) while the rate constant tends to become constant at its higher concentrations. The similar observation of the decrease in rate constant with increasing concentrations of MnO_2 under pseudo-first-order reaction conditions has also been observed for the oxidative degradation of a number of pesticides and other organic compounds, such as glycyl–glycine [27], glycolic acid [28], DL-malic acid [29], metribuzin [31], L-methionine [32], thiourea [35], tricyclazole [36], etc. This behavior of MnO_2 as observed by the present authors as well as by other investigators as described above is against the existing hypothesis of concentration independency of the first-order rate constant. The continuous and regular decrease in rate constant with increasing concentration of MnO_2 is due to possible flocculation of its particles.

The effect of concentration of $HClO_4$ (in range of 1.0×10^{-4}–1.2×10^{-3} mol dm^{-3}) was studied by conducting a series of kinetic measurements at the fixed concentration of acephate (5.0×10^{-3} mol dm^{-3}) and

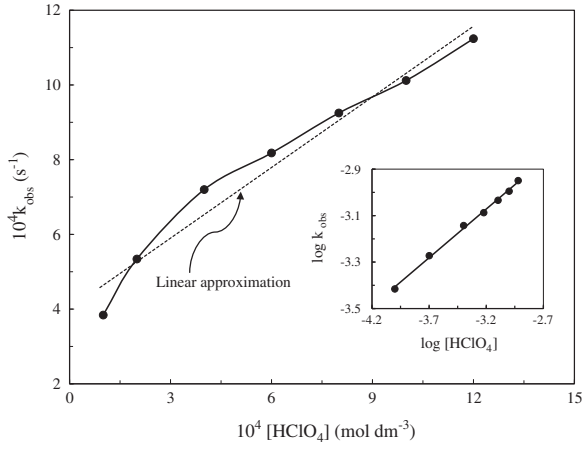

Fig. 4. Effect of $[HClO_4]$ on k_{obs} (inset—effect of log $[HClO_4]$ on log k_{obs}) for the degradation of acephate by colloidal MnO_2 (Reaction conditions: [acephate] = 5.0×10^{-3} mol dm^{-3}, $[MnO_2] = 8.0 \times 10^{-5}$ mol dm^{-3}, temperature = 30 °C).

MnO_2 (8.0×10^{-5} mol dm^{-3}) at a constant temperature of 30 °C. The plot of k_{obs} vs. [$HClO_4$] shown in Fig. 4 clearly indicates that the rate constant increases with increase in [$HClO_4$] throughout the entire observed concentration range (1.0×10^{-4}–1.2×10^{-3} mol dm^{-3}). This figure also indicates that the plot gives a positive intercept on k_{obs} axis under linear approximation ($r^2 = 0.966$). This suggests that the degradation of acephate by colloidal MnO_2 comprises with acid-independent and acid-dependent paths. The nature of rate constant with acid concentration has further been resolved in a better way by making a double logarithmic plot between log k_{obs} and log [$HClO_4$] (Fig. 4—inset). This plot is linear with a slope of 0.419 ($r^2 = 0.997$) which is indicative of fractional-order dependence of the degradation of acephate with respect to [$HClO_4$].

Thus on the basis of above observations and findings, the rate (v) of the degradation of acephate under pseudo-first-order reaction conditions with respect to MnO_2 may be given in term of the following rate law equation:

$$v = -\mathrm{d}[MnO_2]/\mathrm{d}t = (k_I + k_D[HC1O_4]^{0.419})[\text{acephate}]^{0.503}[MnO_2] \quad (2)$$

where k_I and k_D are rate constants for hydrogen ion concentration ([$HClO_4$]) in acid-independent and dependent-paths, respectively.

The acid-independent reaction path taking place may presumably occur by the adsorption of acephate on the colloidal particles of MnO_2 followed by the reaction between adsorbed acephate molecule and one of the MnO_2 molecules pertaining to the colloidal surface leading to the reaction as represented by the following plausible mechanism:

$$\text{Acephate} + (MnO_2)_x \overset{\text{fast}}{\rightleftharpoons} \text{Acephate} - (MnO_2)_x \quad (3)$$

$$\text{Acephate} - (MnO_2)_x \overset{\text{slow}}{\longrightarrow} (MnO_2)_{x-1} + MnO + O - \text{Acephate} \quad (4)$$

where $(MnO_2)_x$ and O-Acephate represent colloidal MnO_2 and intermediate oxidative degrades of acephate (methamidophos, O,S-dimethyl phosphorothioate (DMPT) and O-methyl N-acetylphosphoramidate), respectively.

On the other hand, the acid-dependent path comprises with the adsorption of two hydrogen ions, in addition to acephate molecule, on the colloidal surface of MnO_2 leading to the degradation of acephate by the following plausible mechanism:

$$\text{Acephate} + (MnO_2)_x + 2H^+ \overset{\text{fast}}{\rightleftharpoons} \text{Acephate}-(MnO_2)_x-(H^+)_2 \quad (5)$$

$$\text{Acephate}-(MnO_2)_x-(H^+)_2 \overset{\text{slow}}{\longrightarrow} (MnO_2)_{x-1} + Mn^{2+} + H_2O + O-\text{Acephate} \quad (6)$$

The final smaller degrades of O-Acephate have been observed in the form of non-harmful inorganic ions. The presence of phosphate, nitrate, and sulfate ions in the final reaction mixture has been confirmed by performing the respective qualitative chemical analyses, namely, ammonium molybdate, Devarda's and barium chloride tests. These ions have been assumed to be formed from the decomposition of intermediates methamidophos, DMPT and O-methyl N-acetylphosphoramidate as represented in Fig. 5. Our proposed intermediates and final smaller products are in reasonable agreement with those reported by other investigators under different conditions (Table 1).

3.3. Effect of surfactants

In the present investigation commonly used surfactants such as CTAB (cationic), SDS (anionic), and TX-100 (non-ionic) have been used to study their role on the kinetic behavior of the system. The effect of concentrations of surfactants on the rate constant has been studied at the temperature of 30 °C by keeping the concentration of MnO_2 (8.0×10^{-5} mol dm^{-3}), acephate (5.0×10^{-3} mol dm^{-3}), and $HClO_4$ (6.0×10^{-4} mol dm^{-3}) constant. It has been observed that SDS has no effect on the value of rate constant. This is due to the repulsion between anionic micellar aggregates of SDS (the micelles have net negative charge due to OSO_3^-) and the negatively charged colloidal MnO_2. It is important to note that the water-soluble colloidal MnO_2 in aqueous medium is stabilized by the adsorption of anions resulting in negative charge on its particles [37]. Thereby, the reaction in the presence of CTAB could not be followed well because it possesses positive charge opposite to that of colloidal MnO_2 causing flocculation. Intense turbidity with the clear appearance of precipitates has been observed in reaction mixture. The problem of flocculation has been commonly observed by a number of investigators [24,26–31,36] during their studies on the redox reaction involving colloidal MnO_2 as oxidant in presence of CTAB. However, addition of non-ionic surfactant, TX-100 enhances the rate of reaction. The plots between log (absorbance) vs. time in presence of different concentration of TX-100

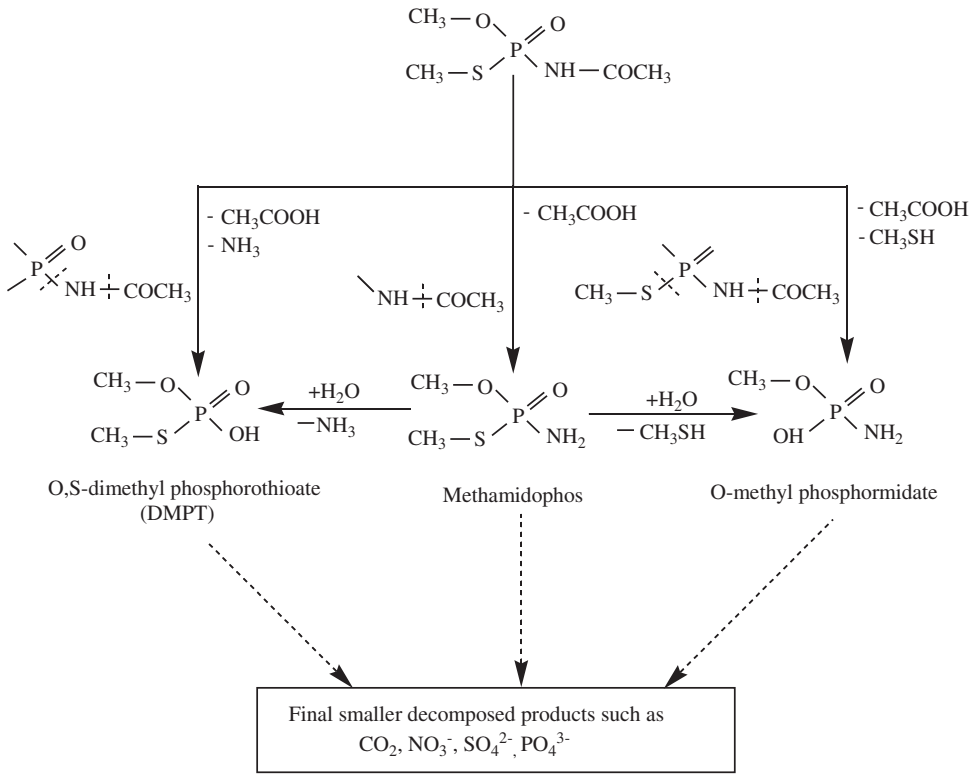

Fig. 5. Proposed pathway for the chemical degradation of acephate by colloidal MnO_2.

Table 1
Degradation of acephate under different conditions

Reaction intermediates	Final degradation products	Reaction conditions	References
$(CH_3O)(CH_3S)P(O)NHCOCH_3$, $CH_3O(CH_3S)P(O)NH_2$, $CH_3O(CH_3S)P(O)OCH_3$, $CH_3O(HO)P(O)OH$, $P(OH)_3$, $CH_3S(O)_2SCH_3$, $(COOH)_2$,	H_3PO_4, CO_2, NO_3^-, SO_4^-, PO_4^{3-}	Photocatalytic degradation of acephate in aqueous TiO_2 suspensions	[17]
Not reported	CO_2, NO_3^-, SO_4^-, PO_4^{3-}, H_2O, H^+	Photocatalytic degradation using UV light and TiO_2 immobilized on silica gel as photocatalyst	[18]
$CH_3O(CH_3S)P(O)OH$, $CH_3O(CH_3S)P(O)NH_2$, along with the elimination of CH_3COOH and NH_4^+	H_3PO_4, CO_2	Biodegradation by a soil bacterium *Pseudomonas aeruginosa* strain Is-6	[20]
$CH_3O(CH_3S)P(O)OH$, $CH_3O(CH_3S)P(O)NH_2$, $CH_3O(OH)P(O)NH_2$ along with elimination of CH_3COOH, NH_3 and CH_3SH	CO_2, NO_3^-, SO_4^{2-}, PO_4^{3-}	Chemical degradation by colloidal MnO_2 in acidic medium	Present investigation

(1.0×10^{-4}–5.0×10^{-3} mol dm^{-3}) were also observed to be linear, as in absence of surfactants, which confirms that the reaction is also first-order with respect to MnO_2 in presence of TX-100. Thus, in other words, the order of reaction with respect to MnO_2 remains the same as that observed in absence of surfactants. The values of pseudo-first-order rate constant (k_ψ) in presence of TX-100 are drawn against [TX-100] in Fig. 6. It is depicted from the figure that the rate constant increases with increasing concentration of TX-100 up to a typical value of 2.0×10^{-3} mol dm^{-3} beyond it remains almost constant on further increase in [TX-100]. However, the catalytic effect is more pronounced in lower concentration range. Tuncay et al.

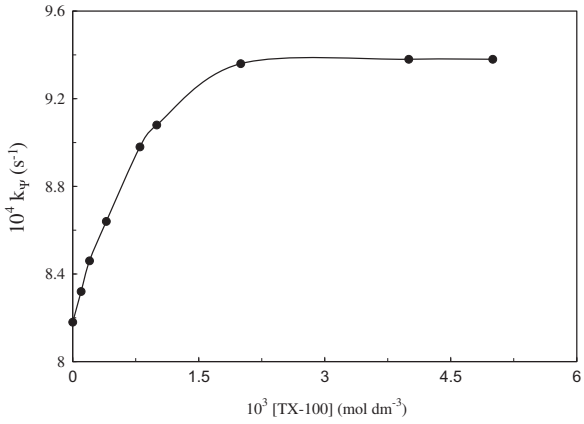

Fig. 6. Effect of [TX-100] on k_ψ for the degradation of acephate by colloidal MnO_2 (Reaction conditions: [acephate] = 5.0×10^{-3} mol dm^{-3}, [MnO_2] = 8.0×10^{-5} mol dm^{-3}, [$HClO_4$] = 6.0×10^{-4} mol dm^{-3}, temperature = 30 °C).

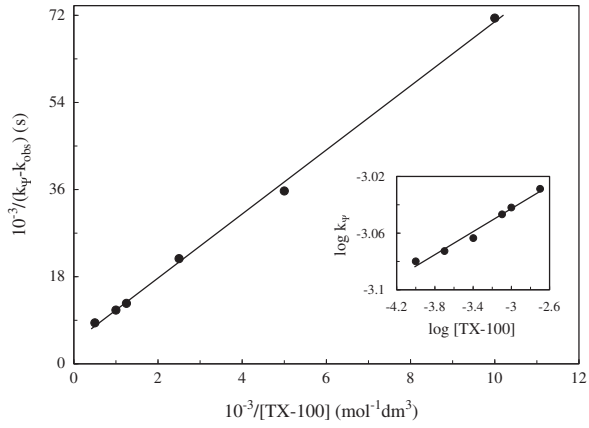

Fig. 7. Plot of $1/(k_\psi - k_{obs})$ vs. 1/[TX-100]) (inset—log k_ψ vs. log [TX-100]) for the degradation of acephate by colloidal MnO_2 (Reaction conditions: [acephate] = 5.0×10^{-3} mol dm^{-3}, [MnO_2] = 8.0×10^{-5} mol dm^{-3}, [$HClO_4$] = 6.0×10^{-4} mol dm^{-3}, [TX-100] = 1.0×10^{-4}–2.0×10^{-3} mol dm^{-3}, temperature = 30 °C).

[24], while studying the kinetics of the reaction between colloidal manganese dioxide and formic acid in aqueous perchloric acid solution, has developed an empirical model to explain the catalytic effect of the surfactant, TX-100. Later on, this model has successfully been used to describe the role of TX-100 for the oxidative degradation of a number of compounds by colloidal MnO_2 by different investigators [26–31,36]. According to this concept, the rate constant (k_ψ) in presence of this surfactant has to obey the following relationship:

$$1/(k_\psi - k_{obs}) = a + b/[\text{TX}{-}100] \quad (7)$$

where a and b are empirical constants. According to the Tuncay concept, the plot of $1/(k_\psi - k_{obs})$ vs. 1/[TX-100] should be linear, which was also observed in the present case for the catalytic concentration range of TX-100 (Fig. 7) with $a = 4{,}493$ s and $b = 6.6178$ mol dm^{-3} s ($r^2 = 0.993$).

In order to further explain the role of TX-100, an alternative empirical equation was also suggested by Tuncay et al. [24]:

$$\log k_\psi = c \log [\text{TX}{-}100] + \text{d} \quad (8)$$

where c and d are other empirical constants. The plot between log k_ψ and log [TX-100] (Fig. 7—inset) was linear which resulted in the value of $c = 0.0406$ and $d = -2.9211$ ($r^2 = 0.980$). The numerical values of these empirical constants strongly depend on the nature and concentration ranges of the reactants as well as reaction conditions. In literature, large variation in the values of these empirical constants has been reported [24,26–31,33,36].

The validity of Eqs. (7) and (8) confirms that the oxidative degradation of acephate by MnO_2 in presence of TX-100 obeys Tuncay model. The catalytic effect of TX-100 is presumably due to the increasing adsorption of reactants in presence of this surfactant. According to Tuncay et al. [24], the driving force for the adsorption of TX-100 is the H-bond formation between polar ethylene oxide and the surface of MnO_2 sols. Furthermore, since adsorption of TX-100 causes a configurational change on the surface of colloidal MnO_2 particles along with the rearrangement of the former molecules on the surface of the latter [24], a complete explanation for the catalytic effect of this surfactant is difficult at present level. However, further work is needed in this direction.

3.4. Effect of temperature on rate constant and determination of activation parameters

A series of kinetic experiments were performed at different temperatures in the range of 20–45 °C at the fixed concentrations of acephate (5.0×10^{-3} mol dm^{-3}), MnO_2 (8.0×10^{-5} mol dm^{-3}), $HClO_4$ (6.0×10^{-4} mol dm^{-3}), and TX-100 (2.0×10^{-3} mol dm^{-3}). The values of rate constant, so obtained at different temperatures, are used to calculate the activation energy of the process. The variation of log k_{obs} against $1/T$ has been observed to obey the following linear relationship ($r^2 = 0.994$) which indicates that the system obeys Arrhenius relationship:

$$\log k_{obs} = -1392/T + 1.5061 \quad (9)$$

The value of activation energy (E_a) as calculated from the slope of the above equation is listed in Table 2. Similarly, the following linear equation ($r^2 = 0.982$) has also been observed for the reaction in the presence of catalyst (TX-100):

$$\log k_\Psi = -1046/T + 0.445 \quad (10)$$

Accordingly, the value of activation energy in presence of TX-100 as obtained from Eq. (10) has also incorporated in Table 2. A lower value of activation energy in presence of surfactant is due to high catalytic effect of TX-100 which provided an alternative path of lower energy barrier for the reaction.

In order to realize whether the reaction mechanism is associative or dissociative, the entropy of activation is necessarily required. The values of entropy of activation ($\Delta S^{\#}$) along with other thermodynamic activation parameters, such as enthalpy of activation ($\Delta H^{\#}$) and free energy of activation ($\Delta G^{\#}$) may be calculated from following Eyring equation:

$$\log (k_{obs} \text{ or } k_\psi/T) = -(\Delta H^{\#}/2.3026\,RT) + \log (k_B/h) + (\Delta S^{\#}/2.3026\,R) \quad (11)$$

In the above equation k_B, R and h represent Boltzman, gas and Plank's constants, respectively. The plot of log (k_{obs}/T) against inverse of temperature ($1/T$) shown in Fig. 8 has resulted in the following linear equation with a very satisfactory correlation coefficient of $r^2 = 0.993$:

$$\log (k_{obs}/T) = -1259/T - 1.412 \quad (12)$$

In a similar way, the following linear equation with $r^2 = 0.976$ has been obtained from log (k_ψ/T) vs. $1/T$ plot:

Table 2
Activation parameters for the degradation of acephate by colloidal MnO_2 (Reaction conditions: [acephate] = 5.0×10^{-3} mol dm^{-3}, [MnO_2] = 8.0×10^{-5} mol dm^{-3}, [$HClO_4$] = 6.0×10^{-4} mol dm^{-3}) and [TX-100] = 2.0×10^{-3} mol dm^{-3})

Activation parameters	Values	
	Aqueous	TX-100
E_a (kJ mol^{-1})	26.7	20.0
$\Delta H^{\#}$ (kJ mol^{-1})	24.1	17.5
$\Delta S^{\#}$ (J K^{-1} mol^{-1})	−224.6	−244.9
$\Delta G^{\#}$ (kJ mol^{-1})	92.2	91.7

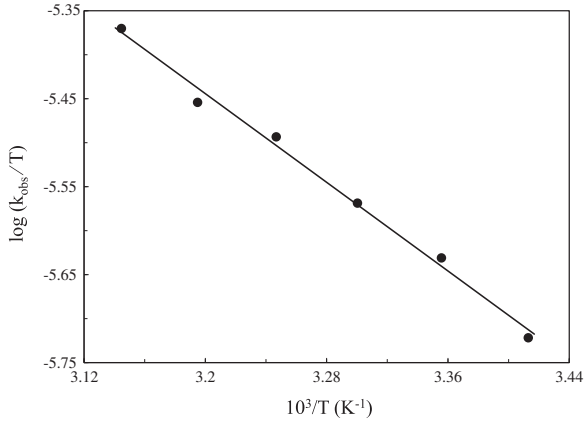

Fig. 8. Eyring plot of log (k_{obs}/T) vs. $1/T$ for the degradation of acephate by colloidal MnO_2 (Reaction conditions: [acephate] = 5.0×10^{-3} mol dm^{-3}, [MnO_2] = 8.0×10^{-5} mol dm^{-3}, [$HClO_4$] = 6.0×10^{-4} mol dm^{-3}, temperature = (293–318 K).

$$\log (k_\psi/T) = -914/T - 2.473 \quad (13)$$

The above results obviously prove that the system obeys Eyring relationship in the absence as well as in the presence of non-ionic surfactant TX-100. The values of different activation parameters for the degradation of acephate by colloidal MnO_2, as calculated from the slope and intercept of the Eqs. (12) and (13), are also presented in Table 2. This table clearly highlights that the contribution of entropy factor is much higher than the enthalpy factor towards the free energy of activation i.e. overall process-controlling parameter. A large negative value of entropy of activation is presumably due to the freezing of translational, rotational, and vibrational degrees freedom on going from ground state to activated-transition state. The negative value of entropy of activation points out the formation of highly ordered associative transition state complex during the degradation process of acephate by colloidal MnO_2. Therefore, the transition state in the region of activated complex has more ordered and rigid reactants than in the ground state. Furthermore, a still higher negative value of entropy of activation in presence of TX-100 is due to increased adsorption as already discussed.

4. Conclusions

The kinetic studies for the oxidative degradation of acephate by colloidal MnO_2 in acidic medium ($HClO_4$) have successfully been performed in the absence and presence of surfactants. The rate constants have been determined as function of the concentrations of

acephate, MnO_2, and $HClO_4$ under the pseudo-first-order reaction conditions. The order of the reaction has been observed to be first order in MnO_2 and fractional order in both acephate and $HClO_4$. On the basis of variation of the rate constant with the concentrations of reactants, the following rate law equation has been developed:

$$v = -\mathrm{d}[MnO_2]/\mathrm{d}t = (k_I + k_D[HC1O_4]^{0.419})[\text{acephate}]^{0.503}[MnO_2] \quad (14)$$

The observed result indicates that the degradation of acephate by MnO_2 occurs via its adsorption over the surface of colloidal particles of the latter. Effect of three common surfactants, namely, cationic CTAB, anionic SDS, and non-ionic TX-100 on the degradation kinetics of acephate by colloidal MnO_2 has also been studied. The anionic surfactant, SDS, has been observed to be ineffective whereas non-ionic surfactant, Triton X-100 (TX-100) accelerates the reaction rate. However, the cationic surfactant, CTAB, causes flocculation with oppositely charged colloidal MnO_2 and therefore could not be studied further. The catalytic effect of TX-100 has been discussed in the light of the available mathematical model. The kinetic results have also been used to generate various activation parameters associated with the degradation of acephate by colloidal MnO_2 in presence of $HClO_4$. The results confirm that the degradation process occurs via the formation of highly ordered compact rigid transition state activated complex.

Acknowledgments

The authors are grateful to the Chairman, Department of Applied Chemistry, Faculty of Engineering and Technology, Aligarh Muslim University for providing necessary laboratory facilities. One of the authors (Qamruzzaman) is also thankful to the University Grants Commission, New Delhi for the award of Maulana Azad National Fellowship.

References

[1] S.Y. Szeto, J. Lee, M.J. Brown, P.C. Oloffs, Simplified methods for determining acepahte and methamidophos residues in several substrates, J. Chromatogr. A 240 (1982) 526–531.
[2] M. Mahajna, G.B. Quistad, J.E. Casida, Acephate insecticide toxicity: Safety conferred by inhibition of the bioactivating carboxyamidase by the metabolite methamidophos, Chem. Res. Toxicol. 10 (1997) 64–69.
[3] J.V. Rao, K. Srikanth, S.K. Arepalli, V.G. Gunda, Toxic effect of acephate on paramecium caudatum with special emphasis on morphology, behaviour, and generation time, Pestic. Biochem. Physiol. 86 (2006) 131–137.
[4] A.T. Farag, M.H. Eweidah, S.M. Tayel, A.H. El-Sebae, Developmental toxicity of acephate by gavage in mice, Reprod. Toxicol. 14 (2000) 241–245.
[5] S.M. Tripathi, A.M. Thaker, C.G. Joshi, L.N. Sankhala, Acephate immunotoxicity in white leghorn cockerel chicks upon experimental exposure, Environ. Toxicol. Pharmacol. 34 (2012) 192–199.
[6] J.S. Osterberg, K.M. Darnell, T.M. Blickley, J.A. Romano, D. Rittschof, Acute toxicity and sub-lethal effect of common pesticides in post-larval and juvenile blue crabs, J. Exp. Mar. Biol. Ecol. 424–425 (2012) 5–14.
[7] M.F. Rahman, M. Mahboob, K. Danadevi, B.S. Banu, P. Grover, Asssessment of genotoxic effect of comet assay in mice leucocytes, Mutat. Res. 516 (2002) 139–147.
[8] J.G. Zinkl, P.J. Shea, R.J. Nakamoto, J. Callman, Effect of cholinesterases of rainbow trout exposed to acephate and methamidophos, Bull. Environ. Contam. Toxicol. 38 (1987) 22–28.
[9] J.H. Yen, K.H. Lin, Y.S. Wang, Potential of the insecticides acephate and methamidophos to contaminate groundwater, Ecotoxicol. Environ. Saf. 45 (2000) 79–86.
[10] M.C. Wang, Y.H. Liu, Q. Wang, M. Gong, X.M. Hua, Y.J. Pang, S. Hu, Y.H. Yang, Impacts of methamidophos on the biochemical, catabolic, and genetic characteristics of soil microbial communities, Soil Biol. Biochem. 40 (2008) 778–788.
[11] T. Perez-Ruiz, C. Martinez-Lozano, A. Sanz, E. Bravo, Determination of organophosphorus pesticides in water, vegetables and grain by automated SPE and MEKC, Chromatographia 61 (2005) 493–498.
[12] L.K. Chai, N. Mohd-Tahir, S. Hansen, H.C.B. Hansen, Dissipation and leaching of acephate, chlorpyrifos, and their main metabolites in field soil of Malaysia, J. Environ. Qual. 38 (2009) 1160–1169.
[13] R. Rezg, B. Mornagui, S. El-Fazaa, N. Gharbi, Organophosphorus pesticides as food chain contaminants and type 2 diabetes: A review, Trends Food Sci. Technol. 21 (2010) 345–357.
[14] J. Fenik, M. Tankiewicz, M. Biziuk, Properties and determination of pesticides in fruits and vegetables, Trends Anal. Chem. 30 (2011) 814–826.
[15] D. Sud, P. Kaur, Heterogeneous photocatalytic degradation of selected organophosphate pesticides: A review, Crit. Rev. Environ. Sci. Technol. 42 (2012) 2365–2407.
[16] S. Ahmed, M.G. Rasul, R. Brown, M.A. Hashib, Influence of parameters on the heterogeneous photocatalytic degradation of pesticides and phenolic contaminants in wastewater: A short review, J. Environ. Manage. 92 (2011) 311–330.
[17] S.T. Han, J. Li, H.L. Xi, D.N. Xu, Y. Zuo, J.H. Zhang, Photocatalytic decomposition of acephate in irradiated TiO_2 suspensions, J. Hazard. Mater. 163 (2009) 1165–1172.
[18] G.R.M. Echavia, F. Matzusawa, N. Negishi, Photocatalytic degradation of organophosphate and phosphonoglycine pesticides using TiO_2 immobilized on silica gel, Chemosphere 76 (2009) 595–600.
[19] R. Zeng, J. Wang, J. Cui, L. Hu, K. Mu, Photocatalytic degradation of pesticide residues with RE^{3+}-doped nano-TiO_2, J. Rare Earth. 28(8) (2010) 353–356 (Special issue) December.

[20] S. Ramu, B. Seetharaman, Biodegradation of acephate and methamidophos by a soil bacterium *Pseudomonas aeruginosa* strain Is-6, J. Environ. Sci. Health., Part B 49 (2014) 23–34.
[21] Q. Zhou, M. Wanga, J. Liang, Ecological detoxification of methamidophos by earthworms in phaiozem co-contaminated with acetochlor and copper, Appl. Soil Ecol. 40 (2008) 138–145.
[22] L.K. Chai, M.H. Wong, N. Mohd-Tahir, H.C.B. Hansen, Degradation and mineralization kinetics of acephate in humid tropic soils of Malaysia, Chemosphere 79 (2010) 434–440.
[23] J.F. Perez-Benito, C. Arias, A kinetic study of the reduction between soluble (colloidal) manganese dioxide and formic acid, J. Colloid Interface Sci. 149 (1992) 92–97.
[24] M. Tuncay, N. Yuce, B. Arlkan, S. Gokturk, A kinetic study of the reduction of colloidal manganese dioxide by formic acid in aqueous perchloric acid solution in the presence of surface active agents, Colloids Surf., A 149 (1999) 279–284.
[25] Z. Khan, P. Kumar, Kinetics and mechanism of the reduction of colloidal manganese dioxide by D-fructose, Colloids Surf., A 248 (2004) 25–31.
[26] Kabir-Ud-Din, N.H. Zaidi, M. Akram, Z. Khan, Mechanism of the oxidation of D-glucose onto colloidal MnO_2 surface in the absence and presence of TX-100 micelles, Colloid Polym. Sci. 284 (2006) 1387–1393.
[27] M. Akram, M. Altaf, Kabir-Ud-Din, Oxidative degradation of dipeptide (glycyl–glycine) by water soluble colloidal manganese dioxide in the aqueous and micellar media, Colloids Surf., B 82 (2011) 217–223.
[28] Kabir-Ud-Din, S.M.S. Iqubal, Z. Khan, Effect of ionic and non-ionic surfactants on the reduction of water soluble colloidal MnO_2 by glycolic acid, Colloid Polym. Sci. 284 (2005) 276–283.
[29] Kabir-Ud-Din, S.M.S. Iqubal, Reduction of soluble colloidal MnO_2 by DL-malic acid in the absence and presence of nonionic TritonX-100, Colloid Polym. Sci. 283 (2005) 504–511.
[30] Kabir-Ud-Din, S.M.S. Iqubal, Kinetics of the reduction of water soluble colloidal MnO_2 by mandelic acid in the absence and presence of non-ionic surfactant TX-100, Colloid J. 72 (2010) 195–204.
[31] Qamruzzaman, A. Nasar, Kinetics of metribuzin degradation by colloidal manganese dioxide in absence and presence of surfactants, Chem. Pap. 68 (2014) 65–73.
[32] M. Ilyas, M.A. Malik, Z. Khan, A kinetic study of the oxidation of L-methionine by water soluble colloidal MnO_2, Colloid Polym. Sci. 285 (2007) 1169–1173.
[33] Kabir-Ud-Din, W. Fatma, Z. Khan, Effect of surfactants on the oxidation of oxalic acid by soluble colloidal MnO_2, Colloids Surf., A 234 (2004) 159–164.
[34] J.F. Perez-Benito, C. Arias, E. Amat, A kinetic study of the reduction of colloidal manganese dioxide by oxalic acid, J. Colloid Interface Sci. 177 (1996) 288–297.
[35] S.M.Z. Andrabi, Z. Khan, Reduction of water soluble colloidal manganese dioxide by thiourea: A kinetic and mechanistic study, Colloid Polym. Sci. 284 (2005) 36–43.
[36] Qamruzzaman, A. Nasar, Degradation of tricyclazole by colloidal manganese dioxide in the absence and presence of surfactants, J. Ind. Eng. Chem. 20 (2014) 897–902.
[37] J.F. Perez-Benito, E. Brillas, R. Pouplana, Identification of a soluble form colloidal manganese(IV), Inorg. Chem. 28 (1989) 390–392.
[38] F. Mata-Perez, J.F. Perez-Benito, Identification of the product from the reduction of permanganate ion by trimethylamine in aqueous phosphate buffers, Can. J. Chem. 63 (1985) 988–992.